Cell, Vol. 105, 103–113, April 6, 2001, Copyright ©2001 by Cell Press

Structural Basis of the Redox Switch in the OxyR Transcription Factor

Hee-Jung Choi,*§ Seung-Jun Kim,*§ Partha Mukhopadhyay,† Sayeon Cho,* Joo-Rang Woo,* Gisela Storz,† and Seong-Eon Ryu*‡

*Center for Cellular Switch Protein Structure
Korea Research Institute of Bioscience and Biotechnology
P.O. Box 115
Yusong, Taejon 305-600
South Korea

†Cell Biology and Metabolism Branch
National Institute of Child Health and Human Development
National Institutes of Health
Bethesda, Maryland 20892

Summary

The *Escherichia coli* OxyR transcription factor senses H_2O_2 and is activated through the formation of an intramolecular disulfide bond. Here we present the crystal structures of the regulatory domain of OxyR in its reduced and oxidized forms, determined at 2.7 Å and 2.3 Å resolutions, respectively. In the reduced form, the two redox-active cysteines are separated by approximately 17 Å. Disulfide bond formation in the oxidized form results in a significant structural change in the regulatory domain. The structural remodeling, which leads to different oligomeric associations, accounts for the redox-dependent switch in OxyR and provides a novel example of protein regulation by "fold editing" through a reversible disulfide bond formation within a folded domain.

Introduction

The intracellular levels of reactive oxygen species (ROS) are the key determinants of cellular redox homeostasis. Disruptions of this homeostasis, which lead to elevated ROS levels, result in cell damage and have been implicated in various degenerative diseases (Halliwell and Gutteridge, 1999). Normal cellular functions also are controlled by low concentrations of ROS that are transiently generated as secondary messengers (Sundaresan et al., 1995; Lander, 1997). The cellular responses to both high and low ROS levels involve proteins whose activities are regulated by oxidation (Storz et al., 1990; Denu and Tanner, 1998; Lee et al., 1998; Zheng et al., 1998; Jakob et al., 1999; Mannick et al., 1999). Many proteins have ROS-sensitive cysteines that are modified by ROS during oxidative stress (Lander, 1997). The hydrogen peroxide (H_2O_2) modification of the active site cysteine in protein tyrosine phosphatases leads to an inhibition of the enzyme activity and facilitates growth factor signaling by prolonging the phosphorylated state of growth factor receptors (Denu and Tanner, 1998; Lee et al., 1998). While an inhibition of enzyme activity can be achieved by a simple modification of the active site cysteines, an activation of proteins through ROS modification may require a significant structural switch. However, the mechanism of ROS-mediated activation has not been described. The *E. coli* OxyR transcription regulator, a member of the LysR family of bacterial transcription factors, is a prototype for proteins whose function is activated by ROS modification (Storz et al., 1990). The OxyR protein is activated by oxidation by H_2O_2 and then induces the transcription of genes necessary for the bacterial defense against oxidative stress (Storz et al., 1990; Zheng et al., 1998).

The activation of OxyR by H_2O_2 occurs by the formation of an intramolecular disulfide bond between Cys-199 and Cys-208, most likely via the oxidation of Cys-199 to a sulfenic acid intermediate (Zheng et al., 1998). Oxidized OxyR can induce the cooperative binding of RNA polymerase to activate transcription (Tao et al., 1993; Kullik et al., 1995a). DNase I and hydroxyl radical footprinting studies showed that the interaction between the OxyR tetramer and DNA is significantly different between the oxidized and reduced forms (Toledano et al., 1994). Reduced OxyR binds DNA at two pairs of major grooves separated by one helical turn, while oxidized OxyR occupies four consecutive major grooves. The extent of the OxyR footprint and the 2-fold dyad symmetry of the OxyR binding motif indicated that OxyR functions as a dimer of dimers. Biochemical analyses including gel filtration and sedimentation experiments revealed that OxyR forms a tetramer in solution (Kullik et al., 1995b; G. S., unpublished data), although a dimeric form was detected in cross-linking experiments (Tartaglia et al., 1992). Oxidized OxyR is inactivated upon reduction of the Cys-199–Cys-208 disulfide bond, indicating that OxyR functions as a reversible cellular redox switch (Zheng et al., 1998). The reduction process is significantly slower than the oxidation, enabling oxidized OxyR to stay for an extended time under overall-reducing environment inside *E. coli* cells (Åslund et al., 1999; Tao, 1999).

The OxyR protein consists of 305 amino acid residues. The N-terminal domain contains a helix-loop-helix DNA binding motif and is connected to the C-terminal regulatory and oligomerization domain (residues 80–305) by a flexible linker that is sensitive to proteolytic digestion (G. S., unpublished data). The C-terminal domain contains the redox-active cysteines (Cys-199 and Cys-208) that mediate the redox-dependent conformational switch (Kullik et al., 1995a, 1995b). Random mutagenesis studies showed that residues important for oligomerization are also located in the C-terminal domain (Kullik et al., 1995b).

To elucidate the mechanism of the redox-dependent conformational switch in OxyR and to understand the redox kinetics and transcription activation by OxyR, we determined the crystal structures of the C-terminal regulatory domain of OxyR in its reduced and oxidized forms.

‡To whom correspondence should be addressed (e-mail: ryuse@mail.kribb.re.kr).
§These authors contributed equally to this work.

Table 1. Crystallographic Data and Refinement Statistics

A. Data collection and MAD Phasing Statistics

	Native (red)	Native (oxi)	SeMet λ1	SeMet λ2	SeMet λ3	SeMet λ4
Resolution range (Å)	100.0–2.7	100.0–2.3	20.0–2.7	20.0–2.7	20.0–2.7	20.0–2.7
Wavelength (Å)	1.54	1.54	0.9879	0.9794	0.9790	0.9667
Data collection temperature	RT[a]	RT[a]	−170°C	−170°C	−170°C	−170°C
Data coverage (%)	93.3	99.2	96.2	96.6	96.8	97.0
R_{sym}[b](%)	7.8	6.4	6.0	7.3	7.2	7.4
<MAD statistics>						
R_{cullis}[c] (centric/acentric)			—	0.41/0.58	0.52/0.60	0.69/0.75
Phasing power[d] (centric/acentric)			—	2.41/2.16	2.10/1.90	1.18/1.16

B. Refinement statistics

	Native (red)	Native (oxi)
Resolution range (Å)	100.0–2.7	100.0–2.3
Reflections (|F| > 0)	18,097	9,049
Number of non hydrogen atoms (protein/water)	3,244	1,657/59
R factor[e]	24.7%	16.9%
R_{free}[e]	27.8%	21.6%
<Rms deviation from idealites>		
Bond lengths(Å)	0.009	0.008
Angles (°)	1.41	1.44
Dihedral angles (°)	23.5	24.1
Improper angles (°)	0.86	0.93

[a] RT: room temperature (about 25°C).
[b] $R_{sym} = \Sigma\Sigma|I_i(h) - <I(h)>|/\Sigma\Sigma I_h(h)$, where $I_i(h)$ is the ith measurement of reflection h and $<I(h)>$ is the weighted mean of all measurements of h.
[c] R_{cullis}: the rms residual lack of closure error divided by the rms structure factor difference.
[d] Phasing power: the rms heavy atom structure factor divided by the rms residual lack of closure variance.
[e] R factor $= \Sigma_h| |F_{obs}(h)| - |F_{calc}(h)| |/\Sigma_h|F_{obs}(h)|$; R_{free} is calculated with 5% of the total data not included in the refinement.

The crystal structures revealed that the reversible disulfide bond formation between distantly located cysteines introduces large structural changes within the regulatory domain. From the structure of the reduced form, we found that the redox-active Cys-199 has a positively charged environment increasing the reactivity of the cysteine sulfur atom. The unique environment of Cys-199 explains the exquisite OxyR sensitivity to H_2O_2. In the oxidized form, the environment of the redox-active cysteine is changed completely allowing OxyR to stay in the activated state for an extended time. The relative rotations between monomers in dimeric and tetrameric associations explain the different DNA binding footprints observed for the reduced and oxidized forms of OxyR. Our results suggest that disulfide bond formation between redox-sensitive cysteines can lead to a large structural switch, which may efficiently regulate protein function, and that the disulfide bond exchange process can be used as a mechanism to modify a protein fold in the middle of a folded domain.

Results and Discussion

Structure Determination

For the crystallization, we used a regulatory domain construct (residues 80–305) whose nonconserved cysteines (Cys-143, Cys-180, and Cys-259) were replaced by alanines (Zheng et al., 1998). These cysteine-to-alanine substitutions do not affect the activity of OxyR (Zheng et al., 1998). The crystals of the reduced form were grown from the regulatory domain with the redox-active Cys-199 residue also mutated to a serine. The C199S mutation locks the protein in the reduced conformation (Kullik et al., 1995a). The structure of the reduced form was determined at 2.7 Å resolution by the multiwavelength anomalous diffraction (MAD) method (Hendrickson and Ogata, 1997) using a crystal grown from selenomethione (Se-Met) substituted protein (Table 1). The crystallization of the oxidized form was achieved from the regulatory domain that has two intact redox-active cysteines (Cys-199 and Cys-208). The structure of the oxidized form was determined at 2.3 Å resolution by the molecular replacement method using the reduced form structure for the search model (Table 1). The reduced and oxidized form structures were refined at 2.7 Å and 2.3 Å resolutions, respectively (Table 1).

Overall Structure

The reduced form monomer of the OxyR regulatory domain consists of two α/β domains that are linked by two interdomain strands (Figure 1A). Residues 87–162 (strands β1–β4, helices αA–αB) form the majority of the N-terminal α/β domain (domain I). The C-terminal α/β domain (domain II) is made of residues 164–260 (strands β5–β10, helices αC–αD). The remaining C-terminal 30 residues come back to domain I to form an edge of the domain (strand β11 and helix αE). The two domains exhibit a similar folding pattern consisting of a central β sheet flanked by helices and loops. The redox-active Cys-199 residue (mutated to a serine for the reduced form structure determination), which reacts with H_2O_2 directly, resides in a narrow hydrophobic pocket between two α/β domains. The second redox-active cysteine (Cys-208) is located at the lower part of domain II

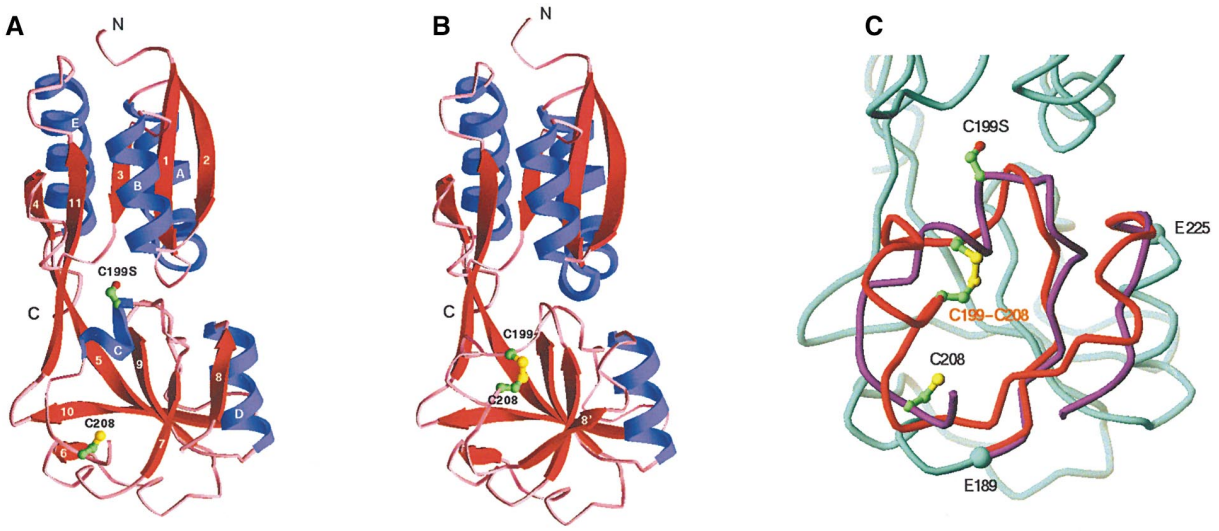

Figure 1. Structure of the OxyR Regulatory Domain

The schematic ribbon diagrams of the OxyR monomers in the reduced (A) and oxidized (B) forms are shown with the redox-active cysteines Cys-199 (C199S in the reduced form) and Cys-208 in a ball-and-stick representation. The β strands and α helices are shown in red and blue, respectively. Secondary structural elements are labeled in the reduced form (A); the boundaries are β1 (92–98), β2 (120–126), β3 (143–145), β4 (156–160), β5 (162–169), β6 (180–182), β7 (190–193), β8 (219–222), β9 (238–241), β10 (254–260), β11 (264–272), αA (102–116), αB (129–138), αC (199–203), αD (224–233), and αE (279–293). The newly created β strand (β8′) is labeled in the oxidized form (B).

(C) Superposition of the reduced and oxidized monomers. Two structures are drawn as superposed by using residues whose Cα carbons can be aligned within a rms of 3.80 Å. Domain II regions are enlarged to show the structural differences clearly. The overall rms value is 0.69 Å for the alignment of 186 residues. Cα carbons of residues 196–221 cannot be aligned within 3.80 Å and are not inculed in the alignment. The reduced and oxidized forms of the residues 189–225 region are shown in purple and red, respectively. For the rest of the molecule, which has very good superposition, only the reduced form is drawn (cyan). The redox-active cysteines are shown in a ball-and-stick representation.

and separated from Cys-199 by a large distance (Figure 1A). The regulatory domains of other bacterial transcription factors, including LacR (Friedman et al., 1995; Lewis et al., 1996), PurR (Schumacher et al., 1994), and CysB (Tyrrell et al., 1997), also are comprised of two α/β domains with the ligand binding sites located at the interface of the two domains. CysB belongs to the LysR family of transcriptional regulators like OxyR, and the monomeric structure of CysB (Tyrrell et al., 1997) is most similar to that of OxyR. A total of 167 C_α carbon atoms of the reduced OxyR monomer can be aligned with corresponding residues of CysB monomer with an rms deviation of 1.84 Å.

The new disulfide bond between the distant cysteines Cys-199 and Cys-208 in the oxidized form monomer "edits" the fold of domain II resulting in a significant rearrangement of secondary structures (Figure 1B). The structural changes encompass one entire face of domain II. First, the residues 199–203, which form a short helix (αC) in the reduced form covering one face of the central β sheet, are looped out. Second, the side chain of Cys-199 is flipped out from the interdomain pocket. Third, the extended strand (β8) made of residues 219–222 becomes a pseudo-helical loop. Fourth, the flexible and solvent exposed loop made of residues 212–217 becomes a new β strand (β8′) and forms an edge of the central β sheet of domain II. When the two structures are superposed by using Cα carbons that can be aligned within an rms of 3.80 Å, the residues between Glu-189 and Glu-225 show the major structural differences and Cα carbons of residues 196–221 cannot be aligned within 3.80 Å (Figure 1C). Despite the dramatic refolding of the redox-active region (residues 189–225), both structures do not show any notable patches of exposed hydrophobic surface. Surfaces that lose hydrophobic interactions due to the structural transition are repacked with other hydrophobic interactions after the transition.

Monomeric Structure Transition

In the reduced form, helix αC containing the redox-active Cys-199 (Ser-199 in the crystal) is stabilized mainly by hydrophobic interactions of Leu-200 with Leu-224 and Pro-241 (Figure 2A). The charge interaction of an ionized Cys-199 with Arg-266 should also contribute to the stability of the region as well as increase the reactivity of the cysteine thiol group by lowering its pKa (see below). For the reduced-to-oxidized form transition, these hydrophobic and charge interactions have to be broken. Interestingly, the side chain of Cys-199 in the reduced form is directed toward the interior of the interdomain pocket, whereas the side chains of the active site cysteines in other redox-related proteins point outwards (Weichsel et al., 1996; Choi et al., 1998). The putative sulfenic acid intermediate first formed upon Cys-199 oxidation by H_2O_2 may not be stable in the pocket due to the limited space and the overall hydrophobic environment made of Ile-98, Val-101, and Ala-147. This unfavorable interaction may drive the oxidized cysteine out of the pocket. However, the flipped-out Cys-199 still has to find the disulfide partner Cys-208 that is separated by about 17 Å (Figure 2A). The flexibility of the 205–216 region may play an important role in bringing Cys-208 to the proximity of the oxidized Cys-199 for the formation of a disulfide bond. In the reduced

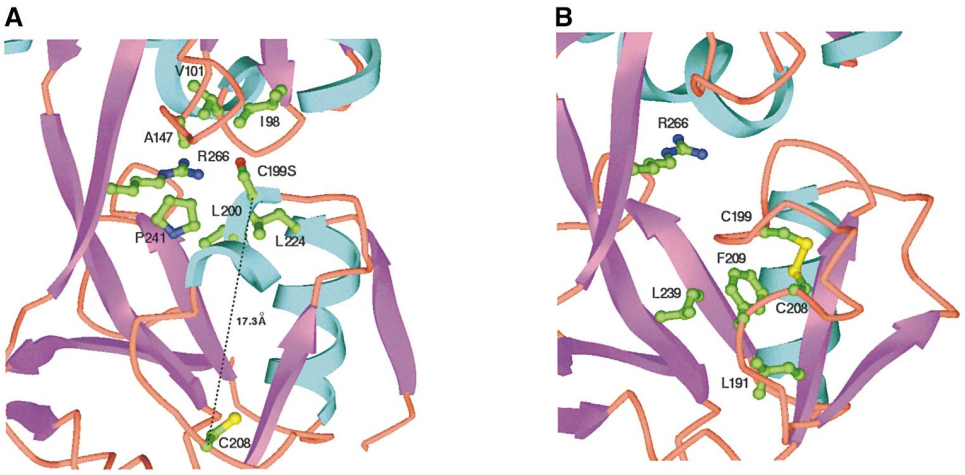

Figure 2. Structural Transition within Monomer

The environment of the redox-active cysteines in the reduced (A) and oxidized (B) forms of OxyR. The redox-active cysteines Cys-199 (Ser-199 in the reduced form) and Cys-208, and the neighboring residues, are shown in a ball-and-stick representation on a ribbon diagram of the region. The point of view is approximately from the left side of the monomers presented in Figure 1.

form structure, the 205–210 region is weakly associated with the main body of the molecule and loosely covers the hydrophobic residues of the central β sheet. In addition, the 211–216 region is not visible in the electron density map. Thus, the 205–216 region is likely to be flexible in solution. The 200–216 region was disordered in the initial refinement of the reduced form by using the data set collected in a synchrotron with a frozen crystal. Later, another native data set collected at room temperature enabled us to define conformations of residues 200–210 (Figure 3A), although the B factor of the 205–210 region was still high. It is likely that the crystal lattice shrinkage during the freezing affected the flexible loop structure that resides in the crystal contact. The flexibility of the loop region might allow Cys-199 to be in an outward conformation a fraction of the time. Cys-199 in this outward conformation would be accessible to other modifications that could lead to partial activation, which may explain why OxyR shows some activation by S-nitrosothiols (Hausladen et al., 1996).

Once the disulfide bond between the two cysteines is formed in the oxidized form, the structure of the 205–216 region is highly stabilized (Figures 2B and 3B). In the oxidized form structure, Phe-209, which is in the flexible loop in the reduced form structure, makes a tightly packed hydrophobic core with Leu-191 and Leu-239 of the central β sheet (Figure 2B). The lack of proper side chain interactions of Phe-209 may result in abnormal conformation changes in the oxidized form. The observation that F209A and F209R mutations confer partial H_2O_2 sensitivity and lead to reduced *oxyS* induction by H_2O_2 confirms the importance of the side chain interactions of Phe-209 in OxyR activation (Table 2). The existence of the disulfide bond is crucial for the maintenance of the structural stability in the oxidized form. First, the disulfide bond holds the 199–208 region in a unique conformation protruding from the main body of the molecule. Second, the disulfide bond covers the newly made hydrophobic core comprised of the redox-active loop and residues of the central β sheet. When the disulfide bond is cleaved by cellular reductants such as glutaredoxin (Zheng et al., 1998), the loop structure and the hydrophobic core should be destabilized and OxyR should go back to the reduced form conformation. As discussed below, the transition from the oxidized to the reduced form may be less efficient than the reduced to

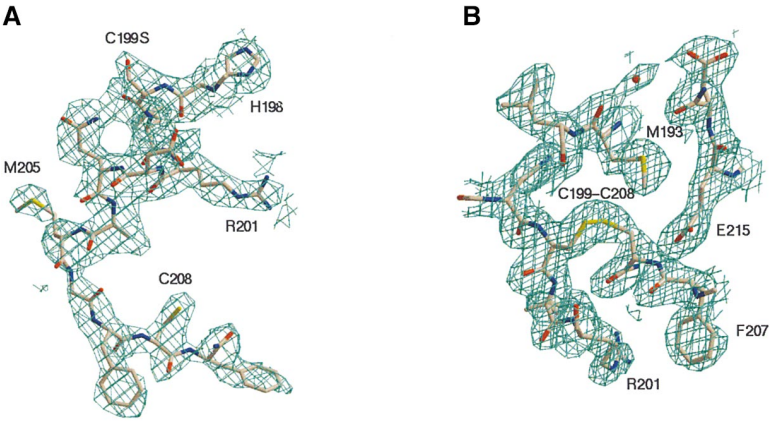

Figure 3. Electron Density Maps of the Redox-Active Cysteine Region

The 2Fo−Fc maps of the reduced (A) and oxidized (B) forms are superposed with the refined models. The maps are contoured at a 0.9 σ level.

Table 2. In Vivo Activity of OxyR Mutants

Mutant	H_2O_2 Sensitivity[a]	*oxyS* RNA Induction[b]		*oxyR-lacZ* Repression[c]
		− H_2O_2	+ H_2O_2	
Vector (pUC18)	36	1.0	1.4	620
Wild-type	23*	1.5	400	44
R266A	27	2.6	140	54
F209A	26	1.4	150	55
F209R	26	1.8	140	43
I110D	23*	94	200	480
L124D	40	3.0	2.3	360
H218D	29	1.2	140	48
F219A	27	1.9	33	44
Δ200–207	18	24	36	35

[a] Total diameter of the zone of growth inhibition (mm) caused by the addition of H_2O_2. An asterisk indicates the presence of a second, larger zone of partial growth. Values are the average of three separate experiments.
[b] Primer extension assay of *oxyS* mRNA levels (normalized to the expression of the nonregulated *bla* gene) in untreated and H_2O_2-treated cells. Values are from a representative experiment and are relative to the levels in the untreated pUC18 control strain.
[c] β-galactosidase assay of *oxyR-lacZ* repression (in Miller units) in untreated cells. Values are the average of assays of two colonies.

oxidized form transition. Nevertheless, the redox-dependent conformational transition in OxyR monomer occurs by alternating between two stable structures. Disruption of each structure either by oxidation of Cys-199 in the reduced form or reduction of the disulfide bond in the oxidized form is likely to force OxyR to seek an alternative structure. The flexibility of the residues 205–216 loop region in the reduced form also appears to play an important role in the structural transition.

Differential Redox Kinetics

In the reduced form, the redox-active Cys-199 residue (Ser-199 in the crystal) makes a close contact with the positively charged side chain of Arg-266 that resides within one side of the interdomain pocket (Figure 2A). The distance between the NE atom of Arg-266 and the oxygen atom of Ser-199 is 5.4 Å, but in the wild-type protein, the distance between the Cys-199 sulfur atom and the NE atom of Arg-266 could be closer due to the ionization of the cysteine sulfide. The stabilization of the thiolate anion of Cys-199 by the charged interaction should lower the pKa of the sulfide group and play an important role in increasing reactivity of the Cys-199 residue toward H_2O_2. The increased H_2O_2 sensitivity and the impaired H_2O_2-dependent induction of the *oxyS* target gene exhibited by a R266A mutant is consistent with such a role of Arg-266 (Table 2). In the reduced form structure of the OxyR regulatory domain, the side chain of Ser-199 is located in the N terminus of a short α helix made of residues 199–203 (helix αC). In addition, the N termini of two long helices (helices αA and αB) point toward the side chain of Ser-199. The helix dipoles generated by the neighboring helices also should contribute to the formation of a more positively charged environment around the ionizable side chain of Cys-199.

In vivo, the reduction of OxyR is significantly slower than the oxidation (Åslund et al., 1999; Tao, 1999). The dramatically different environment of the Cys-199 side chain between the reduced and oxidized forms can explain the unique kinetics of OxyR. In the oxidized form, the charged group of Arg-266 is distant from the Cys-199 side chain (Figure 2B). Instead, the weakly charged side chain of His-198 is close to Cys-199. There also is no longer a helix dipole around the side chain of Cys-199. The short helix (αC) made of residues 199–203 disappears in the oxidized form due to the loop formation in the region, and the Cys-199 side chain is now distant from the N termini of helices αA and αB. Taken together, when the disulfide bond between Cys-199 and Cys-208 is transiently reduced while maintaining the oxidized form conformation, the ionized sulfide group of Cys-199 cannot be stabilized as efficiently as in the reduced form. The environment of Cys-208 also is not favorable for the stabilization of its ionized sulfide group. In thiol-mediated oxidoreductases, the stabilization of the ionized sulfide group in the reduced cysteine governs the efficiency of the disulfide bond reduction (Kortemme and Creighton, 1995). In the oxidized form, due to the lack of the stabilizing environment for the side chains of both Cys-199 and Cys-208, the disulfide bond between them cannot be efficiently reduced even though the disulfide bond is relatively exposed for the accession of cellular reductants such as glutaredoxin.

Oligomeric Structure Transition

The asymmetric unit of the reduced form crystals contains two OxyR regulatory domain molecules. The two molecules, which are related by a noncrystallographic 2-fold symmetry, form a tightly associated dimer (Figure 4A). The major dimeric interaction in the reduced form is mediated by hydrophobic interactions and main chain hydrogen bonds between helix αD (domain II) of monomer A and helix αA and strand β2 (domain I) of monomer B (Figure 4A). The dimerization buries 1,030 $Å^2$ of surface area from each monomer. There is an open cavity in the center of the reduced form dimer with a diameter of about 8 Å. In the oxidized form crystals, two crystallographic 2-fold related OxyR monomers form a similar dimer with a buried surface area of about 1,103 $Å^2$ (Figure 4B). However, monomers of the oxidized form dimer have a relative rotation of about 30° compared to monomers of the reduced form dimer. The relative rotation between two monomers occurs by a lateral sliding of helix αD (domain II) of monomer A relative to the helix αA and strand β2 (domain I) of monomer B (Figures 4C and 4D).

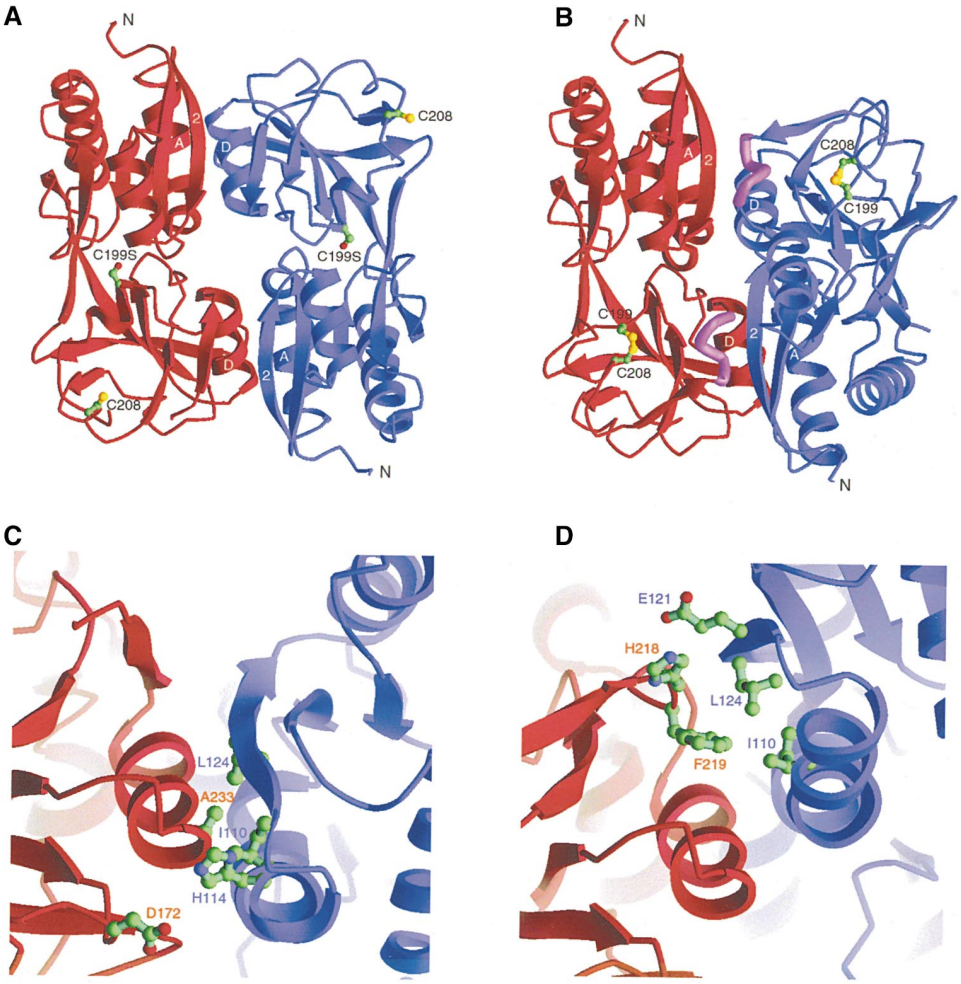

Figure 4. Dimeric Structure

The ribbon diagrams of the OxyR dimer in the reduced (A) and oxidized (B) forms are shown with the redox-active cysteines Cys-199 (C199S in the reduced form) and Cys-208 in a ball-and-stick representation. Two monomers are shown in red (monomer A) and blue (monomer B), respectively. The secondary structural elements in the dimeric interface are labeled. The newly created pseudo-helical loops (residues 218–222) in the oxidized form, which play an important role in the dimeric interactions, are shown as thick, purple lines (B). The left-hand side monomers (red) in the reduced and oxidized forms are presented in a similar orientation to show clearly the relative monomeric rotation of the right-hand side monomer (blue) in the oxidized form. The dimeric interface region in the reduced (C) and oxidized (D) forms are shown. The point of view is from the bottom of the dimers presented in (A) and (B). Two monomers are colored red and blue. Residues important for the dimeric interactions are shown in a ball-and-stick representation. As in (A) and (B), the left-hand side monomers (red) of the reduced and oxidized forms are drawn in a similar orientation.

In the reduced form, Ala-A233 in helix αD forms an intermolecular hydrophobic core with Ile-B110 (helix αA) and Leu-B124 (strand β2), and the side chain of Asp-A172 is close to that of His-B114 for a salt bridge interaction (Figure 4C). After the rotation in the oxidized form, these interactions are broken to make new interacting surfaces. In the oxidized form, helix αD (monomer A) interacts mainly with helix αA (monomer B), and the newly formed pseudo-helical loop (residues 218–222, monomer A) interacts mainly with strand β2 (monomer B) (Figure 4D). Phe-A219 in the loop forms a new hydrophobic core with Ile-B110 and Leu-B124, and a new salt bridge interaction between His-A218 and Glu-B121 is created (Figure 4D). These interactions are possible only after the disulfide bond-mediated structural rearrangements occur. The dimeric association switch appears to be facilitated by a unique arrangement of proline residues (Pro-99, Pro-103, Pro-107, and Pro-111) of helix αA that are aligned in the interaction face of the helix and form a relatively flat helix surface.

The phenotypes of mutants generated by site-directed mutagenesis and isolated in previous genetic screens confirm the importance of the dimeric interactions in the OxyR function. A I110D mutant is resistant to H_2O_2 and shows constitutive expression of the *oxyS* target gene (Table 2), and H114Y and A233V mutants were isolated in a screen for constitutive alleles (Kullik et al., 1995a). We suggest that these mutations destabilize the reduced form dimer while their effects on the oxidized form dimer are minimal. Although Ile-110 is part of the hydrophobic core in the dimeric interface of both forms of OxyR, the I110D mutation may have greater

effects on the reduced form dimer since the side chain of Ile-110 is more exposed in the oxidized form than in the reduced form. In contrast to these mutants, a L124D mutant is extremely sensitive to H_2O_2 and shows almost no *oxyS* induction. We suggest that this mutation destablizes both the reduced and oxidized form dimers. Consistent with a role of the corresponding residues in the reduced form dimeric interactions, the I110D, H114Y, A233V, and L124D mutants all show diminished DNA binding as assayed by repression of the *oxyR* promoter and by DNase I footprinting (Kullik et al., 1995a; Table 2 and data not shown). An interaction with RNA polymerase can restore DNA binding of the A233V mutant in vitro, and presumably the same is true for the I110D and H114Y mutants. Gel filtration experiments showed that the A233V mutation and an E225K mutation, which also is located in the dimeric interface, affect the oligomerization state of OxyR (Kullik et al., 1995b). The side chains of His-218 and Phe-219 only make important dimeric interactions in the oxidized form dimer, and the H218D and F219A mutants show increased sensitivity to H_2O_2 and reduced *oxyS* induction but wild-type repression and DNA binding under reducing conditions (Table 2 and data not shown). These phenotypes are consistent with the H218D and F219A mutations destabilizing only the oxidized form dimer.

Although the regulatory domains appear to be dimers in solution (data not shown), there are interesting tetrameric interactions in both the reduced and oxidized form crystals. For both forms, the structurally switched regions play central roles in the formation of different tetrameric crystal contacts (Figure 5). In the reduced form, two regulatory domain dimers, which are related by a 4-fold screw symmetry, form a tetramer with a side-by-side association of the two dimers (Figure 5A). The screw axis runs through approximately the center of the tetramer in the horizontal direction of the view shown in Figure 5A. The interdimer interactions between the redox loop regions lie in the center of the tetrameric interactions and are related by a noncrystallographic 2-fold symmetry. The structurally switched redox loop region of the oxidized form makes completely different tetrameric crystal contacts (Figure 5B). The two interacting dimers are related by a (1/2, 1/2, 1) translation. The reduced form tetrameric interface between the redox loop regions involves main and side chain interactions between the Met-205 residues from both dimers, and side chain interactions between Met-205 from one dimer and Pro-262 (a cis-proline) from the other dimer (Figure 5C). In addition to the interactions between the redox loop regions, the tetrameric interface involves regions of the interdomain linker strands, strand β4, and the 149–153 and 178–185 loops. In the oxidized form tetramer, the protruding loop made of residues 202–207, which is created by the disulfide bond between Cys-199 and Cys-208, and the residues 210–213 region make contacts with a shallow groove formed by the residues 173–188 region of the interacting molecule (Figure 5D). Currently, there is no direct evidence for the physiological relevance of the regulatory domain tetramers observed in crystals. However, the central role of the redox loop conformation in the switch between the reduced and oxidized form tetramers and the plausible alignment of *oxyS* promoter DNA with the tetramers (see below) indicate that the tetrameric interactions observed in crystals may represent functional interactions of OxyR.

A deletion mutant in which the redox loop (residues 199–208) is replaced by three amino acids (Gln-Gly-Gly) shows increased resistance to H_2O_2 and constitutive *oxyS* expression (Table 2). We propose that this phenotype is caused by the destabilization of the Δ199–208 reduced form tetramer due to the lack of intermolecular interaction between the corresponding loop regions. It is also possible that the deletion mutant mimics the oxidized form by bringing Cys-199 and Cys-208 into close proximity. Our preliminary mutagenesis studies to address the role of specific residues in the tetrameric interactions were not conclusive (data not shown), possibly because tetramerization of the regulatory domain seems to be maintained by many weak interactions at relatively small interfaces. A collection of weak interactions, rather than a few strong interactions, might be required to allow the rapid conformational switch observed for OxyR. In full-length OxyR, other domains, such as the DNA binding domain, also may play a role in maintaining OxyR tetramers. In this context, it is noteworthy that the N-terminal 100 amino acid domain of the nitrogen assimilation control protein (NAC), another member of the LysR family, was found to contain signals for dimerization and transcription activation (Muse and Bender, 1999).

DNA Binding and Transcription Activation

The different dimeric and tetrameric orientations between the reduced and oxidized forms of OxyR have implications for the mechanisms of DNA binding and transcription activation. As a consequence of the relative monomeric rotation in the oxidized form dimer (Figure 4B), N termini of regulatory domains are aligned toward one side of the dimer (the front face in the Figure 4B). This realignment may lead to the rearrangement of the N-terminal DNA binding domains relative to the DNA and thereby facilitate proper DNA binding by oxidized OxyR. Although the observed tetrameric interactions appear to be weak and other interactions may be needed to stabilize the tetramers in solution, the tetameric orientations were consistent with the results of previous footprinting studies (Toledano et al., 1994; Kullik et al., 1995a) when we constructed hypothetical models for the orientation of DNA relative to the tetramers (Figures 5A and 5B). In both the reduced and oxidized form models, the DNA strand lies on the flat face of the OxyR regulatory domain dimers, in agreement with the possible realignment of DNA binding domains toward the flat face of dimers due to the relative monomeric rotation upon oxidation. The reduced form tetramer could be aligned with a DNA stretch of five helical turns with a bend in the third turn. In this complex, two pairs of major grooves are positioned above the regulatory domain in a direction parallel to the monomeric long axis (Figure 5A). The oxidized form tetramer could be aligned with a DNA stretch of four consecutive helical turns. In the oxidized form complex, the DNA runs diagonally to the monomeric long axis (Figure 5B). Thus, the switch from the reduced to oxidized form tetramer seems to be accomplished by a roughly 90° rotation of the right-hand side dimer in Figure 5A, resulting in occupation of different binding sites in DNA.

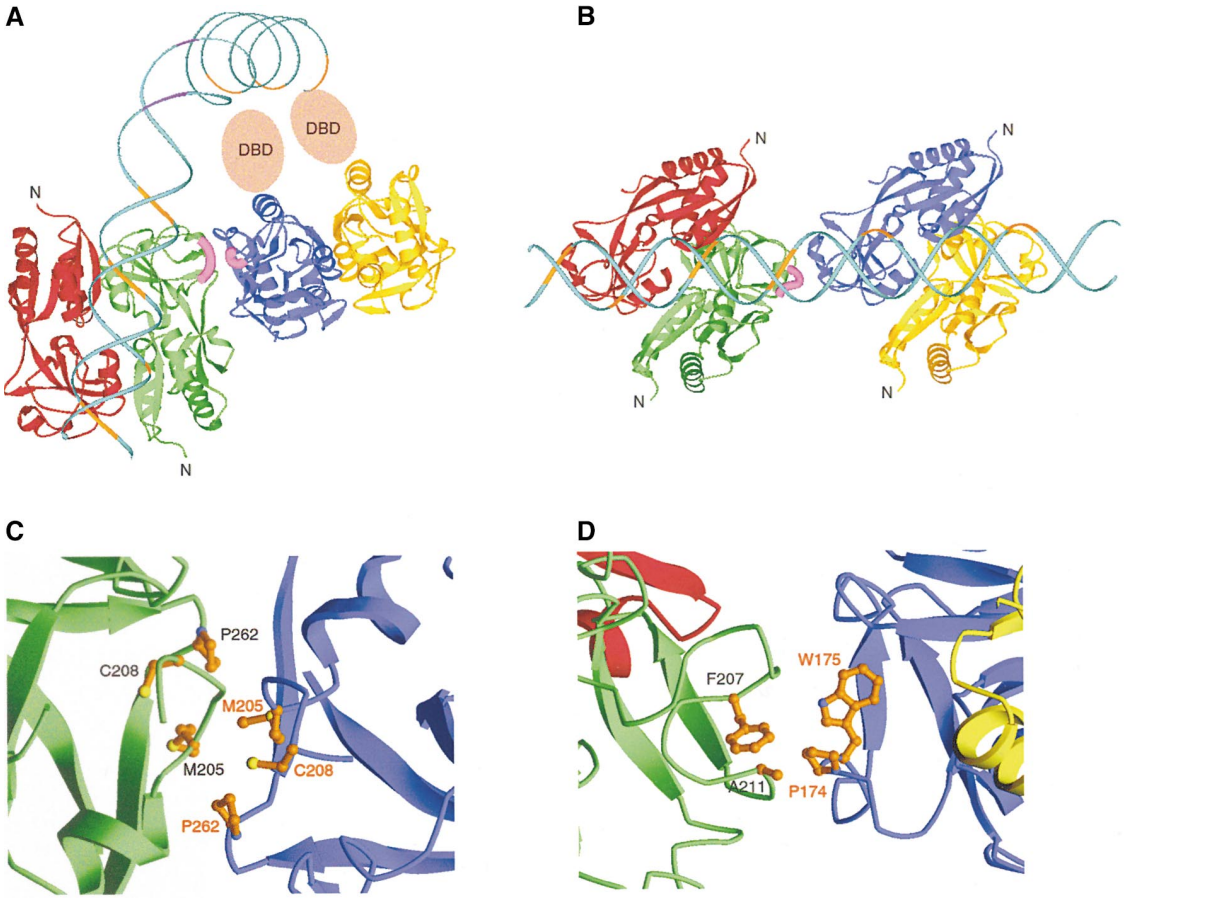

Figure 5. Tetrameric Structure and a Plausible Model of DNA Interactions

The tetramers observed in crystals of the reduced (A) and oxidized (B) forms are shown with the DNA positioned on the tetramers with plausible orientations. The tetramers are shown as ribbons (red, green, blue, and yellow for each monomer) and the model of DNA is represented as helical coils (cyan). The region of *oxyS* promoter DNA (duplex region) protected from DNase I digestion by OxyR binding (Kullik et al., 1995a) was aligned on each regulatory domain tetramer. The DNA bases found to be critical for OxyR binding by the hydroxyl radical missing nucleotide experiment (Toledano et al., 1994) are colored gold. The DNase I hypersensitive sites, which indicate DNA bending in the reduced form (Toledano et al., 1994; Kullik et al., 1995a), are colored purple. The redox loop regions (residues 204–208) of two molecules (molecules colored green and blue) in the reduced form, which play an important role in the tetrameric interaction, are shown as thick, violet lines. The redox loop region of the oxidized form (residues 202–207) in the tetrameric interface is shown as a thick, violet line. The canonical B-DNA stretches were aligned on the tetramers considering the position of the N termini of the respective tetramer where the DNA binding domains of OxyR are expected to be attached. The DNA and the regulatory domains were separated to fit the DNA binding domains (comprised of 80 amino acids each). The possible location of the DNA binding domains (DBD) is indicated for the right-hand side dimer (blue and yellow monomers) of the reduced form. The DNA binding domains of the left-hand side dimer in the reduced form and both dimers in the oxidized form are likely to be located behind the DNA in the space between the DNA and the regulatory domain dimers. The program QUANTA (Molecular Simulations Inc.) was used to create the linear regions of DNA. The bend region of the DNA was modeled from the CAP-DNA complex structure (Schultz et al., 1991). Tetrameric interactions of the reduced (C) and oxidized (D) form tetramers are shown. Side chains of residues important for the tetrameric interactions are shown as a ball-and-stick representation. In the reduced form tetramer, Cys-208 side chains are shown to indicate relative positions of the redox loop residues. The residues in the left-hand side and the right-hand side molecules are labeled in black and red, respectively.

The reorientation of OxyR relative to the DNA due to the different tetrameric orientations also should lead to the presentation of the RNA polymerase contact sites in favorable orientations. In addition, interactions with RNA polymerase appear to be strong enough to induce a conversion to the oxidized form if the reduced form is destabilized. Previous mutagenesis studies identified mutations such as H198R giving rise to mutant proteins that have the reduced form footprint profile under oxidizing conditions (Kullik et al., 1995a). Interestingly, however, proper DNA binding was observed when the H198R protein was incubated with RNA polymerase, and *E. coli* harboring the H198R mutant showed a constitutive activation of OxyR (Kullik et al., 1995a). The side chain of His-198 is partially buried in the domain interface near the redox-active Cys-199 (data not shown), and the introduction of a bulky side chain at the residue 198 position is likely to disrupt the structure of the redox loop region of OxyR. Thus, destablization of the redox loop region may help RNA polymerase induce the proper conformation changes in OxyR to allow oxidized form DNA binding and transcriptional activation. In the activation of the wild-type OxyR, the destabilization of the redox loop region occurs by the steric hindrance of the

oxidized Cys-199 with the side chains inside of the Cys-199 pocket.

Taken together, the cooperative binding of RNA polymerase with the oxidized tetramer seems to be achieved by several different aspects of the OxyR redox switch: the occupation of appropriate DNA binding sites, the presentation of the RNA polymerase interaction surfaces in favorable orientations, and the destabilization of the redox loop regions. Although our model of DNA on the crystallographic tetramers of OxyR explains the previous footprinting results, full understanding of the tetrameric orientation and the mechanisms of transcription activation must await further mutational and functional analyses along with structural studies of OxyR-DNA and OxyR-RNA polymerase complexes.

Implications

Our results show how protein folding and activity can be switched by ROS-mediated disulfide bond formation. The possible regulatory role of a reversible disulfide bond formation in the redox-active proteins had been postulated (Weichsel et al., 1996). However, the disulfide bond-mediated structural changes, which may be needed for efficient regulation of many proteins, had not been shown. Reversible disulfide bond formation in oxidoreductases such as thioredoxin (Weichsel et al., 1996) and DsbA (Guddat et al., 1998) introduces little structural transition since two redox-active cysteines are nearby in the reduced state of these proteins. The reversible fold switch by a disulfide bond formation seen in OxyR provides strong evidence for the postulated potential of the reversible disulfide bond formation in protein regulations. The fold switch also is a novel example of the plasticity of protein structures. Alternative folding of proteins by modification of amino acid residues has been observed for other proteins (Lin et al., 1996; Cordes et al., 1999). The activation of yeast glycogen phosphorylase occurs by a refolding of the N-terminal loop to an α helix upon phosphorylation of a threonine (Lin et al., 1996). A switch mutation between a hydrophobic core residue and an adjacent hydrophilic residue in the N-terminal β strand of Arc repressor leads to an alternative folding of the strand to an α helix (Cordes et al., 1999). The fold switch of the OxyR regulatory domain is unique in that it occurs in the middle of the domain and encompasses one entire face of a folded domain. The introduction of a new covalent bond between two different regions appears to provide the energy required for the large fold switch. The ROS-mediated structural switch in each monomer changes the oligomeric interfaces resulting in a transition in the dimeric and tetrameric associations of OxyR tetramer. Given the potential for achieving large structural rearrangements by joining two domains or two distant regions within one domain, it is likely that other examples of ROS-mediated disulfide bond formation are likely to be found in the future.

Experimental Procedures

Protein Purification

The OxyR regulatory domain (residues 80–305) was amplified from pET11a-OxyR4C→A plasmid (Zheng et al., 1998) by PCR. To keep OxyR in the reduced form, the primary redox-active-residue, Cys-199, was mutated to serine by using the QuikChange site-directed mutagenesis kit (Stratagene). The mutation was confirmed by DNA sequencing. The resulting plasmid was used to transform BL21(DE3) Δ*oxyR::kan* (Zheng et al., 1998). The expressed protein was purified with a combination of ion-exchange (Q-Sepharose and Mono Q), hydrophobic (phenyl superose), and gel filtration (Sephadex G-75) chromatographies. The purification of the reduced and oxidized forms was identical with the exception that 1–2 mM β-mercaptoethanol or DTT was added to the buffers for the reduced form purification. To express the selenomethionine (Se-Met) substituted OxyR protein, the *E. coli* methionine auxotrophic strain B834(DE3) (Novagen) was used. The Se-Met substituted protein was expressed and purified under the same conditions as the native protein.

Crystallization

Crystals of the reduced and oxidized forms of the OxyR regulatory domain were obtained at 25°C by the hanging drop vapor diffusion method. For the crystallization of the reduced form, an aliquot (2 μl) of the protein (30 mg/ml) was mixed with an equal volume of a reservoir solution containing 8%–12% PEG 10 K, 0.2 M CAPS (pH 10.8), 0.1 M benzoic acid, and 0.1 M Tris buffer (pH 8.5). Crystals grew in a tetragonal space group $P4_32_12$ with unit cell dimensions of a = b = 79.49 Å, c = 210.27 Å. Two molecules of the OxyR regulatory domain are in the asymmetric unit of the crystals. Se-Met crystals of the reduced form grew under similar condition. For cryoprotection, Se-Met crystals were transferred into the stabilization solution containing 20% PEG 10 K and 0.1 M sodium cacodylate buffer (pH 6.5). After serial transfer through five steps of increasing glycerol concentration (5% to 25%), the crystals were flash-frozen in liquid nitrogen. To obtain crystals of the oxidized form, hanging drops containing a 1:1 mixture of the protein (2 μl, 20 mg/ml) and reservoir solution (2 μl) were suspended over a reservoir containing 24%–27% PEG 6 K, 0.2 M Li_2SO_4, and 0.1 M Tris buffer (pH 8.5). Crystals grew in a monoclinic space group C2 with cell dimensions of a = 96.83 Å, b = 45.85 Å, c = 53.42 Å, and β = 117.85°. The asymmetric unit of the oxidized form crystals contains one monomer of the OxyR regulatory domain.

Structure Determination and Refinement

A reduced form crystal grown from Se-Met substituted protein was used for the MAD data collection in the beamline X4A at NSLS of Brookhaven National Laboratory equipped with a Quantum 2 × 2 CCD-based detector. Four wavelength data including the edge (λ2), peak (λ3), and two remote wavelengths (λ1, and λ4) were collected at −170°C. Two native data sets for the refinement were collected at room temperature (see text) utilizing a Rigaku RU300 generator with an R-AXIS IIC image plate detector. All data sets were processed with the HKL program suite (Otwinowski and Minor, 1997). Fifteen selenium sites out of total 18 expected sites were located with the program SOLVE (Terwilliger and Berendzen, 1999). The initial electron density map calculated by the MAD phases showed clear solvent boundaries and secondary structural features. The overall figure of merit of the MAD phases was 0.64. The map quality was greatly improved by the solvent flipping/density modification by using the program CNS (Brünger et al., 1998). The resulting map was of high quality to enable the tracing of two entire monomers except for a couple of loop regions. For the structure determination of the oxidized form with the molecular replacement method, the monomer of the reduced form structure was used as the search model. The translation search followed by the rotation search with the program CNS yielded a clear solution that was 5.0 σ above the average peak height.

Refinement of both the reduced and oxidized forms was carried out by using the program CNS. Native data sets for the refinement were collected at room temperature (see text). The randomly selected 5% of data were reserved for the R_{free} calculation. Rounds of refinements were performed with manual rebuildings by using the program O (Jones et al., 1991). In the reduced form, a strong electron density, which was not a part of the protein, was found in the cavity of the dimer center. We modeled it as a benzoic acid that was added for the crystallization. The similar refinement protocols were applied to the oxidized form. The Ramachandran plots drawn by the program PROCHECK (Laskowski et al., 1993) show that 80.5% and 88.3%

of all residues in the reduced and oxidized form structures fall within the most favored regions, respectively. There is no residue in the disallowed regions. The final model in the reduced form includes the residues 87–210 and 217–298 in the first monomer, 87–209 and 216–298 in the second monomer, and one benzoic acid. The final model in the oxidized form includes the residues 87–298 and 59 water molecules. Figures were drawn by using the programs RIBBONS (Carson, 1997) and BOBSCRIPT (Esnouf, 1997).

Mutant Construction and Analysis

pAQ17 (Christman et al., 1989) was mutagenized using the QuikChange site-directed mutagenesis kit. The presence of the mutations and the integrity of the rest of the *oxyR* gene were confirmed by DNA sequencing. TA4112 (RK4936 *oxyRΔ3*, Christman et al., 1985) or MC4100 Δ*oxyR::kan* (λRS45 $O_1O_2O_3O_4O_5$-*lacZ*) (lysogen carrying a *lacZ* fusion to the wild-type *oxyR* promoter, Toledano et al., 1994) carrying pUC18, pAQ17, or the pAQ17 mutant derivatives were grown overnight in Luria Broth medium containing ampicillin (50 μg/ml final concentration) unless indicated. The H_2O_2 resistance of the TA4112 strains was assayed by measuring the zones of growth inhibition around a disk impregnated with 10 μl of 10% H_2O_2 placed in the center of a plate spread with 0.1 ml of cells (Christman et al., 1985). The ability of the TA4112 strains to induce the expression of the *oxyS* target gene was determined by carrying out primer extension assays on total RNA isolated from 15 ml aliquots of a cell culture at OD_{600} = 0.4–0.5, left untreated or treated with 1 mM H_2O_2 for 5 min (Åslund et al., 1999). The relative levels of the primer extension products were quantitated on a phosphoimager (Molecular Dynamics). The ability of wild-type OxyR and the mutant derivatives to function as repressors of the *oxyR* promoter was assayed by measuring the expression of the *oxyR-lacZ* fusion carried by MC4100 Δ*oxyR::kan* (λRS45 $O_1O_2O_3O_4O_5$-*lacZ*). β-galactosidase assays were carried out as described (Toledano et al., 1994) on cultures grown to OD_{600} = 0.5.

Acknowledgments

We are grateful to C. Ogata and the staff at the National Synchrotron Light Source (NSLS) beam line X4A for help with data collection. We thank D.-H. Shin, J.-S. Lee, Y.-J. Choi, and H.-J. Choi for help with the initial characterization of OxyR constructs; J. Hurley, M.-H. Yu, K.-S. Kwon, and S.-S. Kim for comments on the manuscript. This work was supported by a National Creative Research Initiatives grant from the Ministry of Science and Technology, Korea (S.-E. R.) and the intramural program of NICHD (G. S.).

Received December 21, 2000; revised February 9, 2001.

References

Åslund, F., Zheng, M., Beckwith, J., and Storz, G. (1999). Regulation of the OxyR transcription factor by hydrogen peroxide and the cellular thiol-disulfide status. Proc. Natl. Acad. Sci. USA *96*, 6161–6165.

Brünger, A.T., Adams, P.D., Clore, G.M., DeLano, W.L., Gros, P., Grosse-Kunstleve, R.W., Jiang, J.S., Kuszewski, J., Nilges, M., Pannu, N.S., et al. (1998). Crystallography & NMR system: a new software suite for macromolecular structure determination. Acta Crystallogr. *D54*, 905–921.

Carson, M. (1997). Ribbons. Methods Enzymol. *277*, 493–505.

Choi, H.-J., Kang, S.W., Yang, C.-H., Rhee, S.G., and Ryu, S.-E. (1998). Crystal structure of a novel human peroxidase enzyme at 2.0Å resolution. Nat. Struct. Biol. *5*, 400–406.

Christman, M.F., Morgan, R.W., Jacobson, F.S., and Ames, B.N. (1985). Positive control of a regulon for defenses against oxidative stress and some heat-shock proteins in *Salmonella typhimurium*. Cell *41*, 753–762.

Christman, M.F., Storz, G., and Ames, B.N. (1989). OxyR, a positive regulator of hydrogen peroxide-inducible genes in *Escherichia coli* and *Salmonella typhimurium*, is homologous to a family of bacterial regulatory proteins. Proc. Natl. Acad. Sci. USA *86*, 3484–3488.

Cordes, M.H.J., Walsh, N.P., McKnight, C.J., and Sauer, R.T. (1999). Evolution of a protein fold in vitro. Science *284*, 325–327.

Denu, J.M., and Tanner, K.G. (1998). Specific and reversible inactivation of protein tyrosine phosphatases by hydrogen peroxide: evidence for a sulfenic acid intermediate and implications for redox regulation. Biochemistry *37*, 5633–5642.

Esnouf, R.M. (1997). An extensively modified version of MolScript that includes greatly enhanced colouring capabilities. J. Mol. Graph. Model. *15*, 132–136.

Friedman, A.M., Fischmann, T.O., and Steitz, T.A. (1995). Crystal structure of lac repressor core tetramer and its implications for DNA looping. Nature *268*, 1721–1727.

Guddat, L.W., Bardwell, J.C.A., and Martin, J.L. (1998). Crystal structures of reduced and oxidized DsbA: investigation of domain motion and thiolate stabilization. Structure *6*, 757–767.

Halliwell, B., and Gutteridge, J.M.C. (1999). Free Radicals in Biology and Medicine (New York: Oxford University Press).

Hausladen, A., Privalle, C.T., Keng, T., DeAngelo, J., and Stamler, J.S. (1996). Nitrosative stress: activation of the transcription factor OxyR. Cell *86*, 719–729.

Hendrickson, W.A., and Ogata, C.M. (1997). Phase determination from multiwavelength anomalous diffraction measurements. Methods Enzymol. *276*, 494–523.

Jakob, U., Muse, W., Eser, M., and Bardwell, J.C.A. (1999). Chaperone activity with a redox switch. Cell *96*, 341–351.

Jones, T.A., Zou, J.Y., Cowan, S.W., and Kjeldgaard, M. (1991). Improved methods for building protein models in electron density maps and the location of errors in these models. Acta Crystallogr. *A47*, 110–119.

Kortemme, T., and Creighton, T.E. (1995). Ionisation of cysteine residues at the termini of model α-helical peptides. relevance to unusual thiol pKa values in proteins of the thioredoxin family. J. Mol. Biol. *253*, 799–812.

Kullik, I., Toledano, M.B., Tartaglia, L.A., and Storz, G. (1995a). Mutational analysis of the redox-sensitive transcriptional regulator OxyR: regions important for oxidation and transcriptional activation. J. Bacteriol. *177*, 1275–1284.

Kullik, I., Stevens, J., Toledano, M.B., and Storz, G. (1995b). Mutational analysis of the redox-sensitive transcriptional regulator OxyR: regions important for DNA binding and multimerization. J. Bacteriol. *177*, 1285–1291.

Laskowski, R.A., MacArthur, M.W., Moss, D.S., and Thornton, J.M. (1993). PROCHECK: a program to check the stereochemical quality of protein structures. J. Appl. Crystallogr. *26*, 283–291.

Lander, H.M. (1997). An essencial role for free radicals and derived species in signal transduction. FASEB J. *11*, 118–124.

Lee, S.R., Kwon, K.S., Kim, S.R., and Rhee, S.G. (1998). Reversible inactivation of protein-tyrosine phosphatase 1B in A431 cells stimulated with epidermal growth factor. J. Biol. Chem. *273*, 15366–15372.

Lin, K., Rath, V.L., Dai, S.C., Fletterick, R.J., and Hwang, P.K.A. (1996). Protein phosphorylation switch at conserved allosteric site in GP. Science *273*, 1539–1541.

Mannick, J.B., Hausladen, A., Liu, L., Hess, D.T., Zeng, M., Miao, Q.X., Kane, L.S., Gow, A.J., and Stamler, J.S. (1999). Fas-induced caspase denitrosylation. Science *284*, 651–654.

Muse, W.B., and Bender, R.A. (1999). The amino-terminal 100 residues of the nitrogen assimilation control protein (NAC) encode all known properties of NAC from *Klebsiella aerogenes* and *Escherichia coli*. J. Bacteriol. *181*, 934–940.

Lewis, M., Chang, G., Horton, N.C., Kercher, M.A., Pace, H.C., Schumacher, M.A., Brennan, R.G., and Lu, P. (1996). Crystal structure of the lactose operon repressor and its complexes with DNA and inducer. Science *271*, 1247–1254.

Otwinowski, Z., and Minor, W. (1997). Processing of X-ray diffraction data collected in oscillation mode. Methods Enzymol. *276*, 307–326.

Schultz, S.C., Shields, G.C., and Steitz, T.A. (1991). Crystal structure of a CAP-DNA complex: the DNA is bent by 90 degrees. Science *253*, 1001–1007.

Schumacher, M.A., Choi, K.Y., Zalkin, H., and Brennan, R.G. (1994). Crystal structure of LacI member, PurR, bound to DNA: minor groove binding by α helices. Science *266*, 763–770.

Storz, G., Tartaglia, L.A., and Ames, B.N. (1990). Transcriptional regulator of oxidative stress-inducible genes: direct activation by oxidation. Science *248*, 189–194.

Sundaresan, M., Yu, Z.-X., Ferrans, V.J., Irani, K., and Finkel, T. (1995). Requirement for generation of H_2O_2 for platelet-derived growth factor signal transduction. Science *270*, 296–299.

Tao, K. (1999). In vivo oxidation-reduction kinetics of OxyR, the transcriptional activator for an oxidative stress-inducible regulon in Escherichia coli. FEBS Lett. *457*, 90–92.

Tao, K., Fujita, N., and Ishihama, A. (1993). Involvement of the RNA polymerase alpha subunit C-terminal region in co-operative interaction and transcriptional activation with OxyR protein. Mol. Microbiol. *7*, 859–864.

Tartaglia, L.A., Gimeno, C.J., Storz, G., and Ames, B.N. (1992). Multidegenerate DNA recognition by the OxyR transcriptional regulator. J. Biol. Chem. *267*, 2038–2045.

Terwilliger, T.C., and Berendzen, J. (1999). Automated structure solution for MIR and MAD. Acta Crystallogr. *D55*, 849–861.

Toledano, M.B., Kullik, I., Trinh, F., Baird, P.T., Schneider, T.D., and Storz, G. (1994). Redox-dependent shift of OxyR-DNA contacts along an extended DNA-binding site: a mechanism for differential promoter selection. Cell *78*, 897–909.

Tyrrell, R., Verschueren, K.H.G., Dodson, E.J., Murshudov, G.N., Addy, C., and Wilkinson, A.J. (1997). The structure of the cofactor-binding fragment of the LysR family member, CysB: a familiar fold with a surprising subunit. Structure *5*, 1017–1032.

Weichsel, A., Gasdaska, J.R., Powis, G., and Montfort, W.R. (1996). Crystal structure of reduced and oxidized, and mutated human thioredoxins: evidence for a regulatory homodimer. Structure *4*, 735–751.

Zheng, M., Åslund, F., and Storz, G. (1998). Activation of the OxyR transcription factor by reversible disulfide bond formation. Science *279*, 1718–1721.

Protein Data Bank ID Codes

Coordinates for the reduced and oxidized forms of the OxyR regulatory domain have been deposited with the ID codes 1I69 and 1I6A, respectively.